Records of Natural Products

www.acgpubs.org
ORIGINAL ARTICLE

Bioactive compounds from the flowers of *Cannabis sativa* L.: Isolation of a new alkaloid and biological evaluation of cannabinoids and sesquiterpenoids

QuocTuan Nguyen[1], SunHyeong Choi[1], HongDa Yun[1,2], YoungMi Lee[1], ChulMin Kim[3], SeoJeong Oh[4], ManSoo Cho[5], EunSol Lee[6], JungWon Seo[6] and HyunJu Jung[1*]

[1]Department of Oriental Pharmacy, College of Pharmacy and Wonkwang-Oriental Medicines Research Institute, Wonkwang University, Iksan 570-749, Republic of Korea
[2]Korean Ministry of Food and Drug Safety, Osongaengmyeong 2-ro 187, Chungcheongbuk-do 28159, Republic of Korea
[3]Department of Horticulture Industry, Wonkwang University, Iksan 54538, Republic of Korea
[4]College of Pharmacy, Kyung Hee University, Seoul 02447, Republic of Korea
[5]Department of Smart Experience Design, Kookmin University, Seoul 02707, Republic of Korea
[6]Institute of Pharmaceutical Research and Development, College of Pharmacy, Wonkwang University, Iksan 54538, Republic of Korea

Abstract: *Cannabis sativa* L. is a significant plant widely used for both medicinal and recreational purposes. Previous studies have reported that the secondary metabolites of this plant continue to play a crucial role in drug research and development. This study aims to investigate bioactive compounds in the *n*-hexane fraction obtained from the ethanolic extract of *C. sativa* flowers. The isolation yielded eight compounds (**1**–**8**), including one new compound (**1**). Their chemical structures were elucidated by 1D and 2D NMR, HR-ESI-MS, and comparisons with previously reported data. The results of the preliminary biological evaluation revealed that compounds **2**–**4** and **8** suppressed the proliferation of SK-N-SH cells at 10 μM. Notably, compound **4** displayed the strongest activity, with an IC_{50} value of 22.53 ± 1.92 μM, suggesting its potential as a candidate for the development of neuroblastoma cell proliferation inhibitors. In addition, compounds **1**–**8** were also evaluated for antioxidant, tyrosinase, elastase, and collagenase inhibitory activities. Among them, compound **1** showed the highest antioxidant activity, inhibiting 50.89% at 100 μM, compared with ascorbic acid. Compounds **1**–**3** and **6**–**8** also demonstrated elastase inhibitory activity, with inhibition rates ranking from 49.95% to 56.68% at 1 mM, relative to oleanic acid as a positive control. Similarly, compounds **1**, **3,** and **5** inhibited collagenase, with inhibition rates ranging from 55.34% to 73.17% relative to EGCG as a positive control. However, all compounds displayed relatively weak tyrosinase inhibitory effects, with inhibition ranging from 5.22% to 31.02%. This study also represents the first published evaluation of the inhibitory activities of isolated compounds from *C. sativa* flowers against tyrosinase, elastase, and collagenase.

Keywords: *Cannabis sativa*; *Cannabinoids*, SK-N-SH cells, tyrosinase, elastase, collagenase

Cite this article as:
Nguyen et al. Bioactive compounds from the flowers of *Cannabis sativa* L.: Isolation of a new alkaloid and biological evaluation of cannabinoids and sesquiterpenoids. (2026). *Records of Natural Products*, 20(2):e25093648

Received: *28 September 2025*
Revised: *24 October 2025*
Accepted: *12 December 2025*
Published: *05 January 2026*

1 Introduction

The genus *Cannabis* (Family Cannabaceae) comprises three species: *Cannabis indica*, *C. sativa*, and *Cannabis ruderalis* (Pollio, 2016; Schluttenhofer & Yuan, 2017; Kanabus et al., 2021; Pellati et al., 2018). Among them, *C. sativa* is a dioecious plant widely distributed worldwide. It has been recognized as a traditional medicinal ingredient and as a psychoactive medication (Pellati et al., 2018). *C. sativa* has chemical constituents, the most well-characterized of plant species (Taglialatela-Scafati et al., 2010). According to many studies, the phytochemical composition of *C. sativa* includes cannabinoids, flavonoids, stilbenoids, terpenoids, alkaloids, and lignans (Flores-Sanchez & Verpoorte, 2008). Cannabinoids are considered the major chemical components in *C. sativa*, with approximately 120 compounds identified (Schurman et al., 2020; Qian et al., 2024). These

*Corresponding Author: HyunJu Jung. Email: hyun104@wku.ac

are classified into 11 groups based on their structure (García-Gutiérrez et al., 2020). They are terpene phenolic compounds that exert pharmacological activity. Specifically, Δ^9-tetrehidrocannabinol (THC) was found at 4.1% in the *n*-hexane fraction and 7.8% in the acetyl acetate fraction (Tapia-Tapia et al., 2024). It has been shown to inhibit cell proliferation and migration, and to slow tumor progression in mice by inhibiting the AKT and MAPK pathways (Leelawat et al., 2022). *C. sativa* extract rich in cannabinoids has been considered potentially useful in the treatment of Alzheimer's disease (Mooko et al., 2022) and in the protection against oxidative damage (Kopustinskiene et al., 2022). In fact, the products rich in psychoactive THC can be used for both medicinal and recreational purposes (Pellati et al., 2018). Scientific data also reported that cannabidiol (CBD) is a potential compound for the treatment of analgesic, neuroprotective, anticonvulsant, antiemetic, spasmolytic, and anti-inflammatory conditions (Kopustinskiene et al., 2022). In addition, CBD has also been evaluated as a potential new drug for the treatment of psychiatric and anxiety-related disorders (García-Gutiérrez et al., 2020). In addition, the compounds belonging to the cannabinoid family, such as cannabichromene (CBC), cannabigerol (CBG), cannabinol (CBN), tetrahydrocannabivarin (THCV), tetrahydrocannabinolic acid (THCA), cannabidavarin (CBDV), and cannabidiolic acid (CBDA), have demonstrated a wide range of therapeutic effects. These include antioxidant, anti-inflammatory, anticonvulsant, antipsychotic, antifungal, anticancer, antidepressant, antierythemic, analgesic, antibiotic, anticonvulsant, immunomodulatory, neuroprotective, antineoplastic, and antiemetic properties (Odieka et al., 2022). However, in addition to cannabinoids, terpenes have also garnered significant interest from scientists (LaVigne et al., 2021). These terpenes have been evaluated for their biological activities through *in vitro* studies, animal models, and clinical trials. They have shown potential for a variety of therapeutic effects, including anti-inflammatory, antioxidant, analgesic, anticonvulsive, anticancer, and antitumor activities (Nuutinen, 2018; Lowe et al., 2021). In our previous studies, we identified several cannabinoid compounds with strong inhibitory effects on neurblastoma cells, isolated from the ethyl acetate fraction of *C. sativa* (Nguyen et al., 2025). Recognizing the therapeutic potential of these cannabinoids, we extended our investigation to the *n*-hexane fraction to identify additional compounds with inhibitory activity against neuroblastoma cells. Here, we report the isolation of cannabinoids, alkaloids, and sesquiterpenoids from the *n*-hexane fraction of the ethanol extract obtained from the flowers of *C. sativa*. These compounds were evaluated for antioxidant, antitumor, anti-tyrosinase, anti-elastase, and anti-collagenase activities.

2 Materials and Methods

2.1 Plant Materials

The flowers of *C. Sativa* were collected in 2023 from Nongboo Mind Co., Ltd., Korea, and were identified by Prof. Chul Min Kim (Division of Horticulture Industry, Wonkwang University). A voucher specimen (WKU-25) has been deposited at the Pharmacognosy Laboratory, College of Oriental Medicine, Wonkwang University, Chon-bukllo, Korea.

2.2 Cell Culture

Human neuroblastoma SK-N-SH cells were obtained from the Korean Cell Line Bank (Seoul, Korea). The cells were cultured in Minimal Essential Medium (MEM; Gibco, Carlsbad, CA, USA) supplemented with 10% heat-inactivated fetal bovine serum (FBS; Gibco), 100 units/mL penicillin G, and 100 mg/mL streptomycin (Gibco) at 37°C in a humidified atmosphere containing 5% CO_2. Cells were seeded into 96-well plates at a density of 5×10^4 cells/mL. All experiments were conducted 24 hours after cell seeding.

2.3 DPPH Radical Scavenging Assay

The spectrophotometric DPPH (2,2-diphenyl-1-picrylhydrazyl) radical scavenging assay was conducted to evaluate the antioxidant activity of the isolated compounds (Hering et al., 2023). Briefly, 20 µL of each test compound (**1–8**) and the standard ascorbic acid, all at a concentration of 100 µM, were mixed with 80 µL of DPPH solution (200 µM in methanol) in a 96-well microplate. The mixture was incubated at 37°C for 30 minutes in the dark. The absorbance was measured at 517 nM using a microplate reader. The control consisted of 80 µL of DPPH solution and 20 µL of methanol. Ascorbic acid was used as a positive control. DPPH radical scavenging activity was calculated according to the following equation:

$$\text{DPPH inhibition } (\%) = \left(\frac{A_{control} - A_{sample}}{A_{control}} \right) \times 100\%$$

where:

$A_{control}$ is the absorbance value of the control reaction (without inhibitor)

A_{sample} is the absorbance value of the test compound (with inhibitor).

2.4 Cell Viability Assay

Cell viability was assessed in a 96-well plate using a colorimetric 3-[4,5-dimethylthiazol-2-yl]-2,5-diphenyltetrazolium bromide (MTT) assay, which measures mitochondrial activity in living cells. Briefly, SK-N-SH cells were incubated with various concentrations of the compounds (2.5–10 µM) or DMSO for 24 hours, followed by incubation with MTT (1 mg/mL) for 3 hours at 37°C. After incubation, the MTT solution was gently removed, and 100 µL of DMSO was added to each well to dissolve the dark-blue formazan crystals formed by viable cells. Absorbance was measured at 540 nM using a microplate ELISA reader (BioTek Epoch, Vermont, USA). Cell viability in DMSO-treated cells was defined as 100%.

http://doi.org/10.25135/rnp.2509.3648
Rec. Nat. Prod. 2026, 20(2):e25093648

2.5 Tyrosinase Inhibitory Assay

The tyrosinase inhibition assay was conducted as previously described (Kim et al., 2017; Yang et al., 2022). Briefly, 130 µL of tyrosinase (approximately 46 units/mL) prepared in 0.05 mM phosphate buffer (pH = 6.8), was added to each well of a 96-well microplate. Then, 20 µL of each test compound (1 mM) was introduced. Afterward, the enzymatic reaction was initiated by adding 50 µL of 1.5 mM L-tyrosine substrate (also prepared in phosphate buffer). The reaction mixtures were incubated at room temperature, and absorbance was monitored at 475 nM for 20 min using a UV-Vis spectrophotometer.

The tyrosinase inhibitory activity was calculated using the following formula:

$$\text{Inhibition activity rate}\,(\%) = \left(\frac{A_{control} - A_{sample}}{A_{control}}\right) \times 100\%$$

where:

$A_{control}$ is the absorbance value of the control (without inhibitor)

A_{sample} is the absorbance value of the sample (with inhibitor).

2.6 Elastase Inhibitory Assay

The elastase inhibition assay was conducted as previously described (Kim et al., 2024) with slight modifications. Briefly, 140 µL of 0.1M Tris-HCl buffer (pH = 8.0) was added to each well of a 96-well microplate. Then, 20 µL of each test compound (1 mM) and 20 µL of elastase (0.34 unit/mL) were incubated at 25°C for 15 minutes. Then, 20 µL of *N*-succinyl-Ala-Ala-Ala-*p*-nitroanilide (1 mM prepared in Tris-HCl buffer) was added, and the mixture was further incubated at 25°C for 20 minutes. The absorbance was recorded at 410 nM using a UV-Vis spectrophotometer for 30 min at 60s intervals.

The elastase inhibitory activity was calculated using the following formula:

$$\text{Inhibition activity rate}\,(\%) = \left(\frac{A_{control} - A_{sample}}{A_{control}}\right) \times 100\%$$

where:

$A_{control}$ is the absorbance value of the control (without inhibitor)

A_{sample} is the absorbance value of the sample (with inhibitor).

2.7 Collagenase Inhibitory Assay

The collagenase inhibitory activity was evaluated as previously described (Kim et al., 2024) with slight modifications. Briefly, 20 µL of 0.5 mM tricine buffer (pH 7.5) was added to each well of a 96-well microplate. Then, 20 µL of each test compound (1 mM) and 20 µL of collagenase (1.0 U/mL, prepared in tricine buffer) were added, followed by incubation at 37°C for 20 minutes. After 20 µL FALGPA (2 mM) was added, the absorbance was recorded at 435 nM using a UV-Vis spectrophotometer maintained at 37°C. EGCG (Epigallocatechin gallate) was used as a positive control, and 50 mM tricine buffer was used as a negative control.

The collagenase inhibitory activity was calculated using the following formula:

$$\text{Inhibition activity rate}\,(\%) = \left(\frac{A_{control} - A_{sample}}{A_{control}}\right) \times 100\%$$

where:

$A_{control}$ is the absorbance value of the control (without inhibitor)

A_{sample} is the absorbance value of the sample (with inhibitor).

2.8 Extraction and Isolation of Compounds

The dried flowers of *C. sativa* (3.2 kg) were extracted twice with ethanol (EtOH, 10 L × 2) at room temperature. The EtOH extracts were concentrated under reduced pressure to yield a brownish slurry (767.0 g). This EtOH extract was suspended in distilled water (1 L) and successively partitioned with *n*-hexane (3 L × 3) and ethyl acetate (EtOAc, 3 L × 3), yielding *n*-hexane (311.4 g) and EtOAc (40.0 g). The *n*-hexane fraction was subjected to silica *gel* column chromatography (10 × 60 cm), eluted with a stepwise gradient of *n*-hexane-EtOAc (4:1, 3:1, 2:1, 1:1, 1:2, v/v) to afford six subfractions (H1-H6). Fraction H5 (26.4 g) was further separated by silica *gel* column chromatography (5 × 30 cm) and using *n*-hexane-EtOAc (1:0 → 1:2, v/v) to give eight subfractions (H5-1 to H5-8).

Fraction H5-1 (13.2 g) was subjected to reversed-phase YMC RP-C_{18} column chromatography (5 × 30 cm), eluted with MeOH-H_2O (1:1→1:5, v/v), to afford six subfractions (H5-1-1 to H5-1-6). Fraction H5-1-4 (0.83 g) was purified by silica *gel* column chromatography (3 × 60 cm), yielding compound **5** (15.0 mg), **6** (20.8 mg), and two subfractions (H5-1-4-1 and H5-1-4-2). Subfraction H5-1-4-2 (120.0 mg) was purified by semi-preparative HPLC using a CAPCELL PAK C18 type MG column (5 µM, 150 × 20 mm) at a flow rate of 4 mL/min. The mobile phase consisted of a MeCN-H_2O gradient (50%–100% MeCN over 60 min), obtaining compounds **8** (10.4 mg, t_R = 45.5 min), **4** (6.0 mg, t_R = 54.0 min), and **2** (19.1 mg, t_R = 55.5 min). The fraction H5-3 (3.0 g) was separated by YMC RP-C_{18} column chromatography (3 × 60 cm), eluted with MeOH-H_2O (4:1, v/v), to yield four subfractions (H5-3-1 to H5-3-4). Fraction H5-3-2 (104.8 mg) was continuously purified by semi-preparative HPLC (CAPCELL PAK C18 type MG, 5 µM, 150 × 20 mm, flow rate 4 mL/min) using a MeOH-H_2O gradient (85%–100% MeOH, over 60 min) to afford compound **7** (43.3 mg, t_R = 41.5 min). min **3** (9.3 mg, t_R = 43.5 min) was isolated from subfraction H5-3-3 (22.8 mg). Lastly, compound **1** (25.0 mg) was obtained from subfraction H5-3-4 (119.0 mg) by silica *gel* column chromatography (3 × 60 cm), eluted with *n*-hexane-EtOAc (1:1, v/v).

2.9 Mosher's Method

The configuration of the C-2 chiral center in compound **1** was determined by Mosher's method (Ohtani et al., 1991; Quang et al., 2018). To a solution of **1** (1 mg) in $CHCl_3$ (1 mL) were added (*R*)-MTPA or (S)-MTPA Cl (5 μL) and 1 mg of 4-dimethylaminopyridine (DMAP). After stirring at ambient temperature for 24 h, the reaction mixture was evaporated to dryness (**1-*S*** or **1-*R***). After drying the solution in the rotavapor, the residue was purified with reverse-phase HPLC (CAPCELL PAK C18 type MG, 150 × 20 mm, 5 μM, 4.0 mL/min, UV detection at 254 nM) using a gradient solvent system (0–50 min: 60%–100% CH_3CN). The *S*-MTPA ester (ester **1S**, 1.3 mg) was eluted at 16.2 min. The identical procedure was carried out to obtain R-MTPA ester (ester **1R**, 1.3 mg), 17.1 min. (see Supplementary data S37).

3 Results and Discussion

3.1 Structure Elucidation of Isolated Compounds

Compound **1** was obtained as a white powder. Its molecular formula was established as $C_{14}H_{19}NO_3$ based on the HRESIMS ion at *m/z* 250.1444 $[M+H]^+$, consistent with the calculated mass of *m/z* 250.1443 (see Supplementary data S1) and corroborated by the ^{13}C NMR data (Table 1). The ^1H and ^{13}C NMR spectra of **1** (Table 1) revealed the presence of five methylene groups at δ_H 1.14 (2H, *m*, H-5), 1.67 (2H, *m*, H-3), 1.98 (2H, *t*, *J* = 7.6 Hz, H-3′), 2.73 (2H, *m*, H-4), and 2.75 (2H, t, *J* = 7.6 Hz, H-4′), corresponding to carbon signals at δ_C 29.0, 30.8, 35.4, 29.4, and 31.4, respectively, which were confirmed by the HMQC spectrum (see Supplementary data S6). In addition, a methine signal appeared at δ_H 3.98 (1H, *s*, H-2), δ_C 65.3; and a methoxy group δ_H 3.66 (3H, *s*), δ_C 55.3. The aromatic region showed signals indicative of a 1,3,5,6-tetrasubstituted aromatic ring: δ_H 6.23 (d, *J* = 2.2 Hz, H-5′), 6.19 (*d*, *J* = 2.2 Hz, H-7′), with corresponding carbon signals at δ_C 146.5 (C-10′), 101.5 (C-5′), 160.8 (C-6′), 101.2 (C-7′), 155.5 (C-8′), 130.0 (C-9′). These assignments were further supported by key HMBC correlations: from H-5′ (δ_H 6.23) to C-4′ (δ_C 31.4), C-7′ (δ_C 101.2), and C-9′ (δ_C 130.0); and from H-7′ (δ_H 6.19) to C-8′ (δ_C 155.5), C-9′ (δ_C 130.0), and C-5′ (δ_C 101.5). The methoxy group was confirmed to be located at the C-6′ position based on the HMBC correlation from the methoxy protons (δ_H 3.66) to C-6′ (160.8). Furthermore, the structure of **1** was further elucidated through 2D NMR experiments, including COSY, HMQC, and HMBC spectra. The combined HMBC and COSY correlations (Figure 1) indicated that a cyclopentane ring was spiro-fused to the 1,2′-position of a (1′H)-quinoline skeleton. Specifically, HMBC correlations were observed from protons H-3′ (δ_H 1.98) and H-4′ (δ_H 2.75) to C-1 (δ_C 49.2), and C-5 (δ_C 29.0). Additionally, correlations from H-5 (δ_H 1.14) to C-3′ (δ_C 35.4), C-1 (δ_C 49.2), and C-2 (δ_C 65.3); H-3 (δ_H 1.67) to C-1 (δ_C 49.2) supported the connectivity (see Supplementary data S7). To determine the absolute configuration at the C-2 position, Mosher's method was performed to prepare both the (*S*)-MTPA and (*R*)-MTPA esters (Ohtani et al., 1991). The differences in proton chemical shifts observed in the NMR spectra

Table 1. ^1H and ^{13}C NMR spectroscopic data of **1** (400/100 MHz in acetone-*d6*, δ in ppm, *J* in Hz)

Position	1	
	δ_H (*J* in Hz)	δ_C
1	–	49.2
2	3.98 (1H, *brs*)	65.3
3	1.67 (2H, *m*)	30.8
4	2.73 (2H, *m*)	29.4
5	1.14 (2H, *m*)	29.0
1′	–	–
2′	–	–
3′	1.98 (2H, *t*, 7.6)	35.4
4′	2.75 (2H, *t*, 7.6)	31.4
5′	6.23 (1H, *d*, 2.2)	101.5
6′	–	160.8
7′	6.19 (1H, *d*, 2.2)	101.2
8′	–	155.5
9′	–	130.0
10′	–	146.5
OCH_3	3.66 (3H, *s*)	55.3

$\Delta\delta = \delta S\text{-}\delta R > 0$ or $\Delta\delta = \delta S\text{-}\delta R < 0$ led to draw an exact conclusion of the absolute configuration at C-2, which was assigned as *R* (see Supplementary data S36). From the above evidence, the structure of **1** was identified as 3′,4′-dihydro-6′-methoxyspiro[cyclopentane-1,2′(1′H)-quinoline]-2*R*,8′-diol, a new natural product (Figure 2).

Seven known compounds (**2**–**8**) were analyzed by NMR spectroscopy (see Supplementary data) and identified by comparison with literature values. These compounds were identified as Δ^9-tetrahydrocannabinol (Δ^9-*trans*-THC) (Marzullo et al., 2020), cannabigerolic acid (CBGA) (Ahmed et al., 2008), Δ^9-tetrahydrocannabinol (Δ^9-*cis*-THC) (Schafroth et al., 2021), 7-*epi*-γ-eudesmol (Raharivelomanana et al., 1998), α-bisabolol (Lim et al., 2021), guaiol (Wu et al., 2022), β-eudesmol (Shindo et al., 2018). These structures were shown in Figure 2.

Compound 2 (Δ^9-Tetrahydrocannabinol (Δ^9-*trans*-THC)): ^1H NMR (400 MHz, $CDCl_3$): δ_H (ppm): 6.14 (1H, *d*, *J* = 1.2 Hz, H-2), 6.27 (1H, *d*, *J* = 1.2 Hz, H-4), 1.37 and 1.90 (each 1H, *m*, H-7), 2.17 (2H, *m*, H-8), 6.31 (1H, *t*, *J* = 1.6 Hz, H-10), 1.68 (3H, *s*, H-11), 1.09 (3H, *s*, H-12), 1.39 (3H, *s*, H-13), 2.43 (2H, *m*, H-1′), 1.56 (2H, *m*, H-2′), 1.31 (2H, *m*,

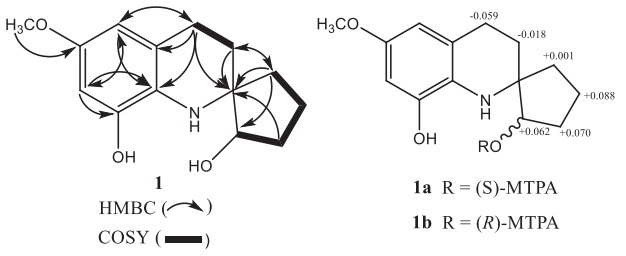

Figure 1. Key HMBC and COSY correlations; and ^1H NMR chemical shift differences of MTPA esters of **1**

http://doi.org/10.25135/rnp.2509.3648
Rec. Nat. Prod. 2026, 20(2):e25093648

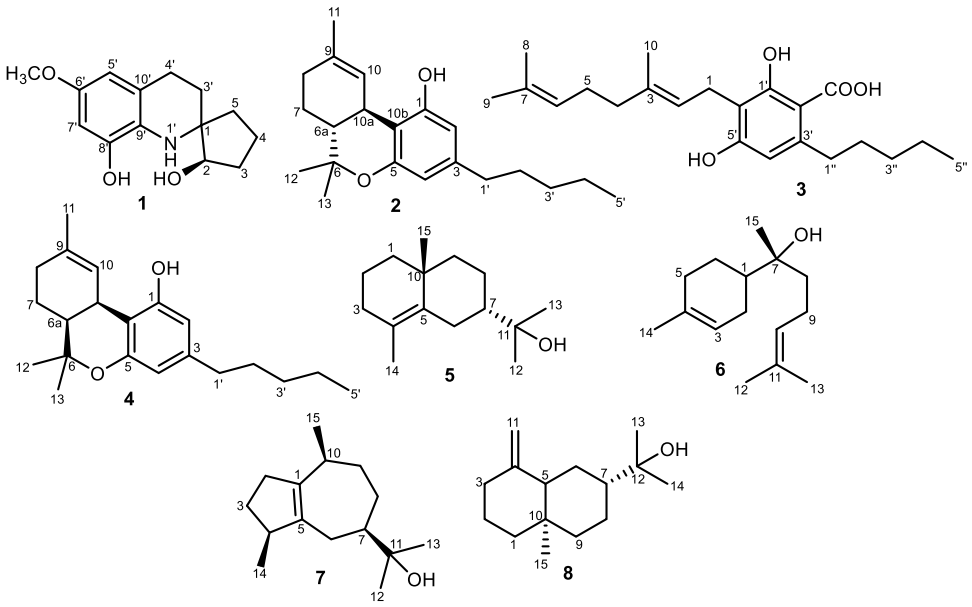

Figure 2. The structure of isolated compounds **1–8**

H-3′), 1.30 (2H, *m*, H-4′), 0.88 (3H, *t*, *J* = 6.8 Hz, H-5′); ^{13}C NMR (100 MHz, $CDCl_3$): δ_C (ppm): 154.3 (C-1), 107.7 (C-2), 142.9 (C-3), 110.2 (C-4), 154.9 (C-5), 77.4 (C-6), 45.9 (C-6a), 25.2 (C-7), 31.7 (C-8), 135.2 (C-9), 123.9 (C-10), 33.7 (C-10a), 109.2 (C-10b), 23.5 (C-11), 19.4 (C-12), 27.7 (C-13), 35.6 (C-1′), 30.8 (C-2′), 31.7 (C-3′), 22.7 (C-4′), 14.2 (C-5′). ESI-MS: *m/z* 315.2319 $[M+H]^+$.

Compound 3 (cannabigerolic acid): ^{1}H NMR (400 MHz, $CDCl_3$): δ_H (ppm): 3.43 (2H, *d*, *J* = 7.2 Hz, H-1), 5.28 (1H, *t*, *J* = 7.2 Hz, H-2), 2.10 (4H, *m*, H-4 and H-5), 5.06 (1H, *t*, *J* = 6.2 Hz, H-6), 1.59 (3H, *s*, H-8), 1.68 (3H, *s*, H-9), 1.82 (3H, *s*, H-10), 2.88 (2H, *t*, *J* = 7.8 Hz H-1″), 1.56 (2H, *m*, H-2″), 1.34 (2H, *m*, H-3″), 1.35 (2H, *m*, H-4″), 0.90 (3H, *t*, *J* = 7.0 Hz, H-5″); ^{13}C NMR (100 MHz, $CDCl_3$): δ_C (ppm): 22.2 (C-1), 121.4 (C-2), 139.4 (C-3), 39.9 (C-4), 26.5 (C-5), 123.9 (C-6), 132.2 (C-7), 17.9 (C-8), 25.8 (C-9), 16.4 (C-10), 163.8 (C-1′), 103.2 (C-2′), 147.5 (C-3′), 111.6 (C-4′), 160.7 (C-5′), 111.4 (C-6′), 36.7 (C-1″), 31.6 (C-2″), 32.2 (C-3″), 22.7 (C-4″), 14.2 (C-5″), 175.3 (CO). ESI-MS: *m/z* 361.2367 $[M+H]^+$.

Compound 4 (Δ^9-Tetrahydrocannabinol (Δ^9-*cis*-THC)): ^{1}H NMR (400 MHz, $CDCl_3$): δ_H (ppm): 6.13 (1H, *brs*, H-2), 6.24 (1H, *d*, *J* = 1.2 Hz, H-4), 1.47 and 1.92 (each 1H, *m*, H-7), 1.97 (2H, *m*, H-8), 6.22 (1H, *m*, H-10), 1.69 (3H, *s*, H-11), 1.27 (3H, *s*, H-12), 1.29 (3H, *s*, H-13), 2.42 (2H, *t*, *J* = 7.8 Hz H-1′), 1.56 (2H, *m*, H-2′), 1.31 (2H, *m*, H-3′), 1.30 (2H, *m*, H-4′), 0.88 (3H, *t*, *J* = 6.8 Hz, H-5′); ^{13}C NMR (100 MHz, $CDCl_3$): δ_C (ppm): 154.0 (C-1), 108.1 (C-2), 142.6 (C-3), 110.1 (C-4), 154.9 (C-5), 76.3 (C-6), 40.2 (C-6a), 20.8 (C-7), 29.9 (C-8), 135.2 (C-9), 122.1 (C-10), 31.6 (C-10a), 109.5 (C-10b), 23.8 (C-11), 25.4 (C-12), 26.1 (C-13), 35.5 (C-1′), 30.7 (C-2′), 31.7 (C-3′), 22.7 (C-4′), 14.2 (C-5′). ESI-MS: *m/z* 315.2316 $[M+H]^+$.

Compound 5 (7-*epi*-γ-eudesmol): ^{1}H NMR (400 MHz, $CDCl_3$): δ_H (ppm): 1.30 and 1.65 (each 1H, *m*, H-1), 1.56 (2H, *m*, H-2), 1.91 (2H, *m*, H-3), 2.11 (1H, *m*, H-6a), 2.72 (1H, *dd*, *J* = 15.2, 2.4 Hz, H-6b), 1.66 (1H, m, H-7), 1.67 (2H, m, H-8), 1.40 (2H, m, H-9), 1.19 (3H, s, H-12), 1.25 (3H, s, H-12), 1.68 (3H, *s*, H-13), 1.09 (3H, *s*, H-15); ^{13}C NMR (100 MHz, $CDCl_3$): δ_C (ppm): 38.2 (C-1), 19.1 (C-2), 39.2 (C-3), 126.1 (C-4), 135.1 (C-5), 25.5 (C-6), 44.2 (C-7), 22.7 (C-8), 39.6 (C-9), 34.6 (C-10), 74.7 (C-11), 28.0 (C-12), 30.0 (C-13), 19.8 (C-14), 26.0 (C-15). ESI-MS: *m/z* 223.2053 $[M+H]^+$.

Compound 6 (α-bisabolol): ^{1}H NMR (400 MHz, $CDCl_3$): δ_H (ppm): 1.56 (1H, *m*, H-1), 1.79 and 2.02 (each 1H, *m*, H-2), 5.37 (1H, *m*, H-3), 1.98 (2H, *m*, H-5), 1.28 (2H, *m*, H-6), 1.66 (1H, *m*, H-7), 1.50 (2H, *ddd*, *J* = 12.4, 7.6, 4.0 Hz, H-8), 2.05 (2H, *m*, H-9), 5.12 (2H, *m*, H-10), 1.68 (3H, *s*, H-12), 1.62 (3H, *s*, H-13), 1.10 (3H, *s*, H-15); ^{13}C NMR (100 MHz, $CDCl_3$): δ_C (ppm): 43.1 (C-1), 27.2 (C-2), 120.7 (C-3), 134.3 (C-4), 31.2 (C-5), 23.4 (C-6), 74.5 (C-7), 40.2 (C-8), 22.2 (C-9), 124.7 (C-10), 131.9 (C-11), 25.9 (C-12), 17.8 (C-13), 23.5 (C-14), 23.3 (C-15). ESI-MS: *m/z* 223.2044 $[M+H]^+$.

Compound 7 (guaiol): ^{1}H NMR (400 MHz, $CDCl_3$): δ_H (ppm): 2.09 and 2.53 (each 1H, *m*, H-2), 1.28 and 1.96 (each 1H, *m*, H-3), 2.53 (1H, *m*, H-4), 1.94 and 2.11 (each 1H, *m*, H-6), 1.52 (1H, *m*, H-7), 1.44 and 1.81 (each 1H, *m*, H-8), 1.57 and 1.70 (each 1H, *m*, H-9), 2.29 (1H, *m*, H-10), 1.16 (3H, *s*, H-12), 1.19 (3H, *s*, H-13), 0.95 (3H, *d*, *J* = 6.8 Hz, H-14), 0.99 (3H, *d*, *J* = 7.2 Hz, H-15); ^{13}C NMR (100 MHz, $CDCl_3$): δ_C (ppm): 140.2 (C-1), 35.5 (C-2), 31.1 (C-3), 46.5 (C-4), 139.0 (C-5), 28.0 (C-6), 49.8 (C-7), 27.4 (C-8), 33.9 (C-9), 33.8 (C-10), 73.8 (C-11), 26.1 (C-12), 27.5 (C-13), 20.1 (C-14), 19.9 (C-15). ESI-MS: *m/z* 223.2062 $[M+H]^+$.

Compound 8 (β-eudesmol): ^{1}H NMR (400 MHz, $CDCl_3$): δ_H (ppm): 1.24 and 1.42 (each 1H, *m*, H-1), 1.57-1.66 (6H, *m*, H-2, H-6, and H-8), 1.99 and 2.30 (each 1H, *m*, H-3), 1.75 (1H, *m*, H-5), 1.34 (1H, *m*, H-7), 1.25 and 1.50 (each 1H, *m*, H-9), 4.44 (1H, *dd*, *J* = 3.2, 1.2 Hz, H-11a), 4.70 (1H, dd, *J* = 3.2, 1.2 Hz, H-11b), 1.20 (6H, *s*, H-13 and H-14), 0.69 (3H, *s*, H-15);

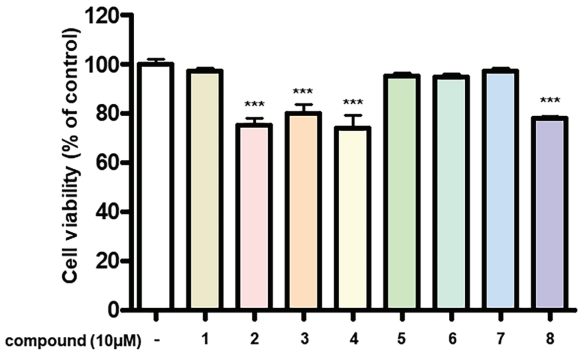

Figure 3. Anti-tumor effects of compounds from *C. sativa* on SK-N-SH neuroblastoma cells. SK-N-SH cells were seeded into 96-well plates at a density of 5 × 10^4 cells/mL and treated with various concentrations of the compounds at 10 μM for 24 hours. Cell viability was determined using the MTT assay, as described in the 'Methods' section. Data represent the means ± standard deviation (S.D.) (n = 3). Statistical significance was determined by one-way ANOVA with Tukey's post hoc test; differences were significant at ***$p < 0.001$ compared to DMSO-treated controls

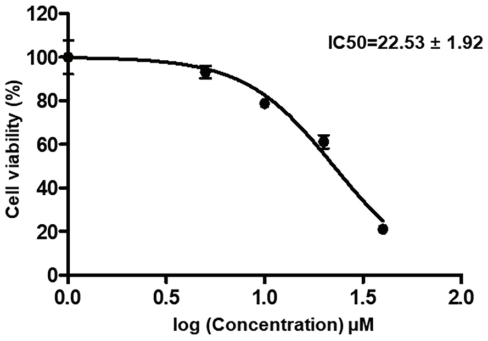

Figure 4. IC_{50} value of **4**

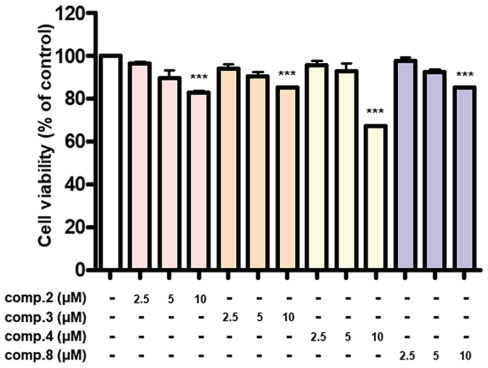

Figure 5. Anti-tumor effects of compounds **2**–**4** and **8** on SK-N-SH neuroblastoma cells. SK-N-SH cells were seeded into 96-well plates at a density of 5 × 10^4 cells/mL and treated with compound **6** at concentrations of 0, 2.5, 5 and 10 μM for 24 hours. Cell viability was assessed using the MTT assay, as described in the 'Methods' section. Data represent the means ± standard deviation (S.D.) (n = 3). Statistical significance was determined by one-way ANOVA with Tukey's post hoc test and differences were statistically significant at ***$p < 0.001$ compared to DMSO-treated controls

^{13}C NMR (100 MHz, $CDCl_3$): δ_C (ppm): 42.0 (C-1), 23.6 (C-2), 37.0 (C-3), 151.3 (C-4), 49.9 (C-5), 22.5 (C-6), 49.5 (C-7), 25.1 (C-8), 41.2 (C-9), 36.0 (C-10), 105.5 (C-11), 73.2 (C-12), 27.2 (C-13), 27.3 (C-14), 16.4 (C-15). ESI-MS: m/z 223.2047 $[M+H]^+$.

3.2 Results of Inhibiting SK-N-SH Neuroblastoma Cells

Neuroblastomas are solid tumors originating in the nervous system and are closely associated with the proliferation of SK-N-SH neuroblastoma cells. Therefore, inhibiting SK-N-SH cell proliferation may contribute to the prevention or treatment of neuroblastoma, a cancer predominantly affecting children (Sun et al., 2023; Ye et al., 2021). In this study, the inhibitory effects of the isolated compounds (**1**–**8**) from *C. sativa* flowers were evaluated against SK-N-SH neuroblastoma cells using the MTT assay. The screening results showed that compounds **2**–**4** and **8** exhibited strong inhibitory effects on SK-N-SH neuroblastoma cells at a concentration of 10 μM (Figure 3). Among them, compound **4** demonstrated the most potent activity, with an IC_{50} value of 22.53 ± 1.92 μM (Figure 4), suggesting that these compounds possess potential antitumor properties. To further investigate their efficacy, the compounds were evaluated at lower concentrations (2.5 and 5 μM). As shown in Figure 5, compounds **2**–**4** and **8** exhibited noticeable inhibitory effects at 5 μM, whereas no significant activity was observed at concentrations below 5 μM. Considering their structural features and biological activities, among all the isolated compounds, the cannabinoids demonstrated the strongest inhibitory effect on the proliferation of neuroblastoma cells.

3.3 Antioxidant Activity of Isolated Compounds

In this study, the antioxidant activity of the isolated compounds was evaluated using the DPPH free radical scavenging assay. As presented in Table 2, all compounds were tested at a concentration of 100 μM. Among the eight isolated compounds (**1**–**8**), compound **1** exhibited the strongest DPPH radical scavenging activity, with an inhibition rate of 50.98 ± 1.38%. Compounds **2**–**5** showed moderate activity, with inhibition rates ranging from 43.21 ± 2.13% to 22.42 ± 3.31%, whereas compounds **6** and **8** displayed negligible or no activity. These findings suggest that the antioxidant activity of the sesquiterpenoid compounds was generally lower than that of the cannabinoid and alkaloid derivatives.

3.4 Tyrosinase Inhibition of Isolated Compounds

Tyrosinase is a critical regulatory enzyme in melanin biosynthesis in melanocytes. It catalyzes the initial steps of melanogenesis, including the hydroxylation of L-tyrosine to L-DOPA and the subsequent oxidation of L-DOPA to dopaquinone (Fan et al., 2021; Klomsakul & Chalopagorn, 2018). However, excessive melanin production can result in hyperpigmentation disorders such as melasma, lentigines, freckles, and, in severe cases, may contribute to the development of melanoma and other genotoxic effects (Klomsakul & Chalopagorn, 2018). Consequently, tyrosinase inhibitors have attracted significant interest in both the cosmetic and

http://doi.org/10.25135/rnp.2509.3648
Rec. Nat. Prod. 2026, 20(2):e25093648

Table 2. Inhibition rate of compounds **1**–**8** on antioxidant, tyrosinase, elastase, and collagenase

Compounds	Inhibition rate (%)[a]			
	DPPH[c]	Tyrosinase[d]	Elastase[d]	Collagenase[d]
1	50.98 ± 1.38	5.22 ± 3.12	50.09 ± 2.51	55.34 ± 4.94
2	43.21 ± 2.13	6.58 ± 1.41	49.95 ± 0.81	19.51 ± 3.87
3	19.81 ± 0.99	21.25 ± 6.00	55.10 ± 1.17	73.17 ± 4.66
4	28.85 ± 1.72	11.16 ± 1.42	43.12 ± 2.22	19.51 ± 4.16
5	22.42 ± 3.31	13.03 ± 1.42	37.85 ± 2.03	59.76 ± 5.01
6	–	31.02 ± 5.79	50.60 ± 2.75	–
7	22.15 ± 0.91	24.98 ± 5.61	56.68 ± 2.80	32.93 ± 4.22
8	–	13.20 ± 4.23	53.94 ± 0.99	–
Kojic acid[b,d]	–	99.55 ± 0.54	–	–
Oleanic acid[b,d]	–	–	81.61 ± 0.45	–
Ascorbic acid[b,c]	70.94 ± 1.19	–	–	–
EGCG[b,d]	–	–	–	79.27 ± 4.28

Note: [a]All experiments were conducted in triplicate; [b]Positive control, [c]at a concentration of 100 μM; [d]at a concentration of 1 mM.

pharmaceutical industries, particularly for their potential as skin-whitening agents and in the treatment of pigmentary disorders (Wawrzyńczak, 2023; Karkoszka et al., 2024). In this assay, the tyrosinase inhibitory activity of isolated compounds **1**–**8** was evaluated *in vitro* using a spectrophotometric method. All compounds were tested at 1 mM, with kojic acid as the positive control. As shown in Table 2, compound **1** exhibited the weakest inhibitory effect (5.22 ± 3.12%), whereas compound **6** demonstrated the strongest activity (31.02 ± 5.79%) relative to the positive control. Since tyrosinase is implicated in neurodegenerative disorders such as Parkinson's disease (Viet et al., 2021; Hasegawa, 2010), its inhibition may help prevent these diseases. In relation to their structural features, the results indicated that the sesquiterpenoid compounds exhibited stronger activity than the other isolated compounds.

3.5 Elastase Inhibition of Isolated Compounds

Elastase is a proteolytic enzyme that degrades components of the extracellular matrix, including elastin. The loss of elastin is a major factor contributing to visible signs of skin aging, such as wrinkles and sagging (Chompoo et al., 2012). Therefore, inhibition of elastase activity may serve as a valuable strategy for protecting against skin aging and related dermatological conditions. In this study, the anti-elastase activity of isolated compounds was evaluated *in vitro* using SANA (*N*-succinyl-Ala-Ala-Ala-*p*-nitroanilide) as the substrate. The assay measured the formation of *p-nitroaniline* at 410 nM, which resulted from SANA hydrolysis by elastase. Oleanic acid was used as a positive control. The results of the enzymatic assay for the isolated compounds (**1**–**8**) are summarized in Table 2. Overall, these compounds exhibited stronger elastase inhibitory activity than tyrosinase inhibition. At a concentration of 1 mM, elastase inhibition ranged from 37.85% to 56.68%, whereas tyrosinase inhibition was lower, ranging from 5.22% to 31.02% (Table 2). Among them, compound **7** demonstrated the highest elastase inhibition, with an inhibition rate of 56.68 ± 2.80%, while compound **5** showed the weakest activity, with an inhibition rate of 37.85 ± 2.03%. Based on structural characteristics, compounds **1**–**3** and **6**–**8** showed higher activity compared to the other compounds.

3.6 Collagenase Inhibition of Isolated Compounds

Collagenases, members of the matrix metalloproteinase (MMP) family, are zinc-dependent transmembrane endopeptidases (Hartmann et al., 2015). Dysregulated collagenase activity can contribute to abnormal MMP expression, which has been linked to a variety of diseases, including neurological disorders such as Parkinson's disease, Alzheimer's disease, Japanese encephalitis, and glaucoma. MMPs are also implicated in conditions such as Crohn's disease and hepatic ischemia (Mustafa et al., 2022). Under normal physiological conditions, MMPs are typically expressed at low levels; however, elevated levels are frequently observed in different cancers and are correlated with enhanced tumor proliferation and progression (Mustafa et al., 2022). In this study, the inhibitory activity of the isolated compounds against collagenase was evaluated. The results are shown in Table 2. Among them, compounds **1**, **3,** and **5** exhibited the strongest collagenase inhibition, with inhibition rates at 55.34%, 73.17% and 59.76%, respectively. Whereas compounds **6** and **8** were inactive.

Cannabis sativa is a highly versatile plant, with its seeds, leaves, roots, stems, and flowers utilized across various industries. These plant parts have shown considerable potential for applications in cosmetics, pharmaceuticals, and human nutrition (Rupasinghe et al., 2020). Moreover, *C. sativa* is recognized as a rich source of bioactive compounds, making it a promising candidate for the development of therapeutic and cosmetic products. Phytochemical investigations have identified a diverse array of constituents

in *C. sativa*, including cannabinoids, terpenes, polyphenols, triterpenes, alkaloids, and essential oils (Hourfane et al., 2023). Among these, cannabinoids and terpenes are regarded as the primary bioactive components. In addition, *C. sativa* exhibits a broad spectrum of biological activities, such as antioxidant, antibacterial, anticoagulant, insecticidal, anticancer, anti-aflatoxigenic, antifungal, cytotoxic, anti-elastase, anti-collagenase, anti-acetylcholinesterase, anti-inflammatory, and neuroprotective effects, such as anti-Alzheimer's, anti-epileptic, and anti-Parkinson's activities (Hourfane et al., 2023). Previous studies have extensively reported the antioxidant activity of *C. sativa* using various *in vitro* assays, including the free radical scavenging method (DPPH), oxygen radical absorbance capacity (ORAC), ferric reducing ability of plasma (FRAP), and 2,20-azino-bis (3-ethylbenzothiazoline-6-sulphonic acid) (ABTS), as well as other methods such as phosphomolybdenum and metal chelation assays (Hourfane et al., 2023). Antioxidant activities of *C. sativa* have been demonstrated in several parts of the plant, including the seeds, leaves, and aerial parts (Hourfane et al., 2023). In this study, we further evaluated the antioxidant activity of compounds isolated from the flowers of *C. sativa* and found that compounds **1**–**5** and **7** exhibited antioxidant activity, whereas compounds **6** and **8** showed negligible or no activity. Similarly, the leaf extracts of *C. sativa*, which are rich in polyphenols and cannabinoids, have also demonstrated strong tyrosinase inhibitory activity, with an IC_{50} value of 0.07 ± 0.06 mg/mL (Manosroi et al., 2019), as well as collagenase and elastase inhibition rates of 80% and 30%, respectively, at a concentration of 1 mg/mL (Zagórska-Dziok et al., 2021). Our findings also demonstrated that the purified compounds, including Δ^9-tetrahydrocannabinol (Δ^9-*trans*-THC) (**2**), cannabigerolic acid (**3**), Δ^9-Tetrahydrocannabinol (Δ^9-*cis*-THC) (**4**), 7-*epi*-γ-eudesmol (**5**), α-bisabolol, (**6**), guaiol (**7**), β-eudesmol (**8**) exhibited inhibitory activity against tyrosinase, elastase, and collagenase, providing valuable data for the screening of potential candidates for skin-improving applications.

4 Conclusion

In this study, the application of various chromatographic techniques for the isolation of compounds from *C. sativa* flowers led to the discovery of one new compound (**1**) and seven known compounds (**2**–**8**). Among these, compounds **2**–**4** and **8** exhibited the most potent inhibitory effect on the proliferation of SK-N-SH neuroblastoma cells, suggesting their potential as candidates for the development of anti-neuroblastoma agents. Furthermore, all isolated compounds were also assessed by DPPH, anti-tyrosinase, anti-elastase, and anti-collagenase assays. These findings indicated that all compounds displayed inhibitory activity against tyrosinase, elastase, and collagenase, except for compounds **6** and **8**, which showed no effect on collagenase. It was thought that *C. sativa* would be a good candidate for both skin and medicine applications.

Funding Statement

This study was supported by a grant from the Rural Development Administration (project No. RS2022RD010270).

Authors Contributions

QuocTuan Nguyen.; Methodology, Formal analysis, Writing-original manuscript., SunHyeong Choi.; Methodology., HongDa Yun.; Validation, Data curation., YoungMi Lee.; Formal analysis., ChulMin Kim.; Formal analysis., SeoJeong Oh.; Visualization., ManSoo Cho.; Visualization, Investigation., EunSol Lee.; Methodology., JungWon Seo.; Writing-review & editing., HyunJu Jung.; Writing-review & editing, Project administration, Conceptualization.

Availability of Data and Materials

The authors declare that the data supporting the findings of this study are available within the paper and its Supplementary Information files. Should any raw data files be needed in another format they are available from the corresponding author upon reasonable request. Source data are provided with this paper.

Ethics Approval

This study involved only *in vitro* biochemical assays and the use of isolated compounds. No human participants or live animals were involved.

Conflicts of Interest

The authors declare that there is no conflict of interest.

Supporting Information

Supporting information accompanies this paper on http://www.acgpubs.org/journal/records-of-natural-products.

ORCID

QuocTuan Nguyen: 0009-0001-6170-5747
SunHyeong Choi: 0009-0008-2118-2743
DaYun Hong: 0009-0002-7359-4914
ChulMin Kim: 0009-0003-5626-7257
SeoJeong Oh: 0009-0009-6700-7892
EunSol Lee: 0009-0006-5594-6778
JungWon Seo: 0000-0002-7613-1053
HyunJu Jung: 0000-0002-2756-0644

References

Ahmed, S. A., Ross, S. A., Slade, D., Radwan, M. M., Zulfiqar, F. & ElSohly, M. A. (2008). Cannabinoid ester constituents from high-potency *Cannabis sativa*. *Journal of Natural Products*, *71*(4), 536–542. DOI: 10.1021/np070454a.

Chompoo, J., Upadhyay, A., Fukuta, M. & Tawata, S. (2012). Effect of Alpinia zerumbet components on antioxidant and skin diseases-related enzymes. *BMC Complementary and Alternative Medicine*, *12*(1), 106. DOI: 10.1186/1472-6882-12-106.

Fan, Y.-F., Zhu, S.-X., Hou, F.-B., Zhao, D.-F., Pan, Q.-S., Xiang, Y.-W., Qian, X.-K., Ge, G.-B. & Wang, P. (2021). Spectrophotometric assays for sensing tyrosinase activity and their applications. *Biosensors*, *11*(290), 290. DOI: 10.3390/bios11080290.

Flores-Sanchez, I. J. & Verpoorte, R. (2008). Secondary metabolism in cannabis. *Phytochemistry Reviews*, *7*(3), 615–639. DOI: 10.1007/s11101-008-9094-4.

García-Gutiérrez, M. S., Navarrete, F., Gasparyan, A., Austrich-Olivares, A., Sala, F. & Manzanares, J. (2020). Cannabidiol: A potential new alternative for the treatment of anxiety, depression, and psychotic disorders. *Biomolecules*, *10*(11), 1575. DOI: 10.3390/biom10111575.

Hartmann, A., Gostner, J., Fuchs, J. E., Chaita, E., Aligiannis, N., Skaltsounis, L. & Ganzera, M. (2015). Inhibition of collagenase by mycosporine-like amino acids from marine sources. *Planta Medica*, *81*(10), 813–820. DOI: 10.1055/s-0035-1546105.

Hasegawa, T. (2010). Tyrosinase-expressing neuronal cell line as in vitro model of Parkinson's disease. *International Journal of Molecular Sciences*, *11*(3), 1082–1089. DOI: 10.3390/ijms11031082.

Hering, A., Stefanowicz-Hajduk, J., Gucwa, M., Wielgomas, B. & Ochocka, J. R. (2023). Photoprotection and antiaging activity of extracts from honeybush (*Cyclopia* sp.)-in vitro wound healing and inhibition of the skin extracellular matrix enzymes: Tyrosinase, collagenase, elastase and hyaluronidase. *Pharmaceutics* *15*(5):1542. 10.3390/pharmaceutics15051542

Hourfane, S., Mechqoq, H., Bekkali, A. Y., Rocha, J. M. & Aouad, N. E. (2023). A comprehensive review on *Cannabis sativa* ethnobotany, phytochemistry, molecular docking and biological activities. *Plants*, *12*(1245), 1245. DOI: 10.3390/plants12061245.

Kanabus, J., Bryła, M., Roszko, M., Modrzewska, M. & Pierzgalski, A. (2021). Cannabinoids—Characteristics and potential for use in food production. *Molecules*, *26*(21), 6723. DOI: 10.3390/molecules26216723.

Karkoszka, M., Rok, J. & Wrześniok, D. (2024). Melanin biopolymers in pharmacology and medicine—Skin pigmentation disorders, implications for drug action. *Adverse Effects and Therapy, Pharmaceuticals*, *17*(521), 521. DOI: 10.3390/ph17040521.

Kim, H.-B., Kim, E.-S., Kim, K. T., Kim, Y.-M. & Eom, S.-H. (2024). *In vitro* study on the inhibitory effects of Korean brown, green, and red seaweed extracts on collagenase, elastase, and hyaluronidase. *Fisheries and Aquatic Sciences*, *27*(11), 783–790. DOI: 10.47853/fas.2024.e72.

Kim, J. H., Yoon, J.-Y., Yang, S. Y., Choi, S.-K., Kwon, S. J., Cho, I. S., Jeong, M. H., Kim, Y. H. & Choi, G. S. (2017). Tyrosinase inhibitory components from *Aloe vera* and their antiviral activity. *Journal of Enzyme Inhibition and Medicinal Chemistry*, *32*(1), 78–83. DOI: 10.1080/14756366.2016.1235568.

Klomsakul, P. & Chalopagorn, P. (2018). *In vitro* antioxidant activity, inhibitory effect of tyrosinase and DOPA auto-oxidation by *Wrightia religiosa* extracts. *South African Journal of Botany*, *120*(2019), 302–308. DOI: 10.1016/j.sajb.2018.09.025.

Kopustinskiene, D. M., Masteikova, R., Lazauskas, R. & Bernatoniene, J. (2022). *Cannabis sativa* L. bioactive compounds and their protective role in oxidative stress and inflammation. *Antioxidants*, *11*(4), 660. DOI: 10.3390/antiox11040660.

LaVigne, J. E., Hecksel, R., Keresztes, A. & Streicher, J. M. (2021). *Cannabis sativa* terpenes are cannabimimetic and selectively enhance cannabinoid activity. *Scientific Reports*, *11*(1), 8232. DOI: 10.1038/s41598-021-87740-8.

Leelawat, S., Leelawat, K., Yimsoo, T., Wunnakup, T., Monton, C., Khamthong, N., Madaka, F., Maha, A. & Songsak, T. (2022). Antitumor effects of delta (9)-tetrahydrocannabinol and cannabinol on cholangiocarcinoma cells and xenograft mouse models. *Evidence-Based Complementary and Alternative Medicine*, *2022*, 6477132. DOI: 10.1155/2022/6477132.

Lim, H. S., Kim, S. K., Woo, S.-G., Kim, T. H., Yeom, S.-J., Yong, W., Ko, Y.-J., Kim, S.-J., Lee, S.-G., & Lee, D.-H. (2021). (−)-α-bisabolol production in engineered *Escherichia coli* expressing a novel (−)-α-bisabolol synthase from the globe artichoke *Cynara cardunculus* var. *Scolymus*. *Journal of Agricultural and Food Chemistry*, *69*(30), 8492–8503. DOI: 10.1021/acs.jafc.1c02759.

Lowe, H., Steele, B., Bryant, J., Toyang, N. & Ngwa, W. (2021). Non-cannabinoid metabolites of *Cannabis sativa* L. with therapeutic potential. *Plants*, *10*(2), 400. DOI: 10.3390/plants10020400.

Manosroi, A., Chankhampan, C., Kietthanakorn, B.-O, Ruksiriwanich, W., Chaikul, P., Boonpisuttinant, K., Sainakham, M., Manosroi, W., Tangjai, T. & Manosroi, J. (2019). Pharmaceutical and cosmeceutical biological activities of Hemp (*Cannabis sativa* L var. *sativa*) leaf and seed extracts. *Chiang Mai Journal of Science*, *46*(2), 180–195.

Marzullo, P., Foschi, F., Coppini, D. A., Fanchini, F., Magnani, L., Rusconi, S., Luzzani, M. & Passarella, D. (2020). Cannabidiol as the substrate in acid-catalyzed intramolecular cyclization. *Journal of Natural Products*, *83*(10), 2894–2901. DOI: 10.1021/acs.jnatprod.0c00436.

Mooko, T., Bala, A., Tripathy, S., Kumar, C. S., Mahadevappa, C. P., Chaudhary, S. K. & Matsabisa, M. G. (2022). *Cannabis Sativa* L. flower and bud extracts inhibited *in vitro* cholinesterases and β-secretase enzymes activities: Possible mechanisms of cannabis use in Alzheimer disease. *Endocrine, Metabolic & Immune Disorders—Drug Targets*, *22*(3), 297–309. DOI: 10.2174/1871530321666210222124349.

Mustafa, S., Koran, S. & AlOmair, L. (2022). Insights into the role of matrix metalloproteinases in cancer and its various therapeutic aspects: A review. *Frontiers in Molecular Biosciences*, *9*, 1101. DOI: 10.3389/fmolb.2022.896099.

Nguyen, T.-Q., Park, H.-S., Choi, S.-H., Hong, D.-Y., Cheon, J.-Y., Lee, Y.-M., Kim, C.-M., Hong, J.-K., Oh, S.-J., Cho, M.-S., Kim, J.-H., Lee, E.-S., Seo, J. & Jung, H.-J. (2025). New cannabinoids and chlorin-type metabolites from the flowers of *Cannabis sativa* L.: A study on their neuroblastoma activity. *Pharmaceuticals*, *18*(4), 521. DOI: 10.3390/ph18040521.

Nuutinen, T. (2018). Medicinal properties of terpens found in *Cannabis sativa* and *Humulus lupulus*. *European Journal of Medicinal Chemistry*, *157*, 198–228.

Odieka, A. E., Obuzor, G. U., Oyedeji, O. O., Gondwe, M., Hosu, Y. S. & Oyedeji, A. O. (2022). The medicinal natural products of *Cannabis sativa* Linn.: A review. *Molecules*, *27*(5), 1689. DOI: 10.3390/molecules27051689.

Ohtani, I., Kusumi, T., Kashman, Y. & Kakisawa, H. (1991). High-Field FT NMR application of Mosher's method. The absolute configurations of marine terpenoids. *Journal of the American Chemical Society*, *113*(34), 4092–4096. DOI: 10.1002/chin.199134221.

Pellati, F., Borgonetti, V., Brighenti, V., Biagi, M., Benvenuti, S. & Corsi, L. (2018). *Cannabis sativa* L. and nonpsychoactive cannabinoids: Their chemistry and role against oxidative stress, inflammation, and cancer. *BioMed Research International*, *2018*(12), 1–15. DOI: 10.1155/2018/1691428.

Pollio, A. (2016). The name of *Cannabis*: A short guide for non-botanists. *Cannabis and Cannabinoid Research*, *1*(1), 234–238. DOI: 10.1089/can.2016.0027.

Qian, L., Beers, J. L., Jackson, K. D. & Zhou, Z. (2024). CBD and THC in special populations: Pharmacokinetics and drug-drug interactions. *Pharmaceutics*, *16*(4), 484. DOI: 10.3390/pharmaceutics16040484.

Quang, T. H., Kim, D. C., Kiem, P. V., Minh, C. V., Nhiem, N. X., Tai, B. H., Yen, P. H., Ngan, N. T. T., Kim, H. J. & Oh, H. (2018). Macrolide and phenolic metabolites from the marine-derived fungus Paraconiothyrium sp. VK-13 with anti-inflammatory activity. *The Journal of Antibiotics*, *71*(9), 826–830. DOI: 10.1038/s41429-018-0073-8.

Raharivelomanana, P., Bianchini, J.-P., Ramanoelina, A. R. P., Rasoarahona, J. R. E., Faure, R. & Cambon, A. (1998). Eudesmane sesquiterpenes from *Laggera alata*. *Phytochemistry*, *47*(6), 1085–1088. DOI: 10.1016/s0031-9422(98)80077-0.

Rupasinghe, H. P. V., Davis, A., Kumar, S. K., Murray, B. & Zheljazkov, V. D. (2020). Industrial Hemp (*Cannabis sativa* subsp. sativa) as an emerging source for value-added functional food ingredients and nutraceuticals. *Molecules*, *25*(4078), 4078. DOI: 10.3390/molecules25184078.

Schafroth, M. A., Mazzoccanti, G., Reynoso-Moreno, I., Erni, R., Pollastro, F., Caprioglio, D., Botta, B., Allegrone, G., Grassi, G., Chicca, A., Gasparrini, F., Gertsch, J. R., Carreira, E. M. & Appendino, G. (2021). Δ^9-cis-tetrahydrocannabinol: Natural occurrence, chirality, and pharmacology. *Journal of Natural Products*, *84*(9), 2502–2510. DOI: 10.1021/acs.jnatprod.1c00513.

Schluttenhofer, C. & Yuan, L. (2017). Challenges towards revitalizing hemp: A multifaceted crop. *Trends in Plant Science*, *22*(11), 917–928. DOI: 10.1016/j.tplants.2017.08.004.

Schurman, L. D., Lu, D., Kendall, D. A., Howlett, A. C. & Lichtman, A. H. (2020). Molecular mechanism and cannabinoid pharmacology. *Handbook of Experimental Pharmacology*, *258*(1), 323–353. DOI: 10.1007/164_2019_298.

Shindo, K., Hattan, J.-I., Kato, M., Sato, M., Ito, T., Shibuya, Y., Watanabe, A., Sugiyama, M., Nakamura, Y. & Misawa, N. (2018). Purification and structural analysis of volatile sesquiterpenes produced by *Escherichia coli* carrying unidentified terpene synthase genes from edible plants of the family *Araliaceae*. *Bioscience, Biotechnology, and Biochemistry*, *82*(6), 978–985. DOI: 10.1080/09168451.2017.1386085.

Sun, S.-Q., Du, F.-X., Zhang, L.-H., Hao-Shi, Gu, F.-Y., Deng, Y.-L. & Ji, Y.-Z. (2023). Prevention of STAT3-related pathway in SK-NSH cells by natural product astaxanthin. *BMC Complementary Medicine and Therapies*, *23*(1), 430. DOI: 10.1186/s12906-023-04267-3.

Taglialatela-Scafati, O., Pagani, A., Scala, F., Petrocellis, L. D., Marzo, V. D., Grassi, G. & Appendino, G. (2010). Cannabimovone, a cannabinoid with a rearranged terpenoid skeleton from hemp. *European Journal of Organic Chemistry*, *11*(11), 2067–2072. DOI: 10.1002/ejoc.200901464.

Tapia-Tapia, E., Aránguiz, P., Diaz, R., Espinoza, L., Caroline, Weinstein-Oppenheimer, R. & Cuellar, M. (2024). Effect of *Cannabis sativa* L. extracts, phytocannabinoids and their acetylated derivates on the SHSY-5Y neuroblastoma cells'viability and caspases 3/7 activation. *Biological Research*, *57*, 33. DOI: 10.1186/s40659.

Viet, T. D., Xuan, T. D. & Anh, L. H. (2021). α-amyrin and β-amyrin isolated from celastrus hindsii leaves and their antioxidant, anti-xanthine oxidase, and anti-tyrosinase potentials. *Molecules*, *26*(7248), 7248. DOI: 10.3390/molecules26237248.

Wawrzyńczak, A. (2023). Cosmetic and pharmaceutic products with selected natural and synthetic substances for melasma treatment and methods of their analysis. *Cosmetics*, *10*(3), 86. DOI: 10.3390/cosmetics10030086.

Wu, C.-C., Huang, S.-L., Ko, C.-H. & Chang, H.-T. (2022). Antifungal sesquiterpenoids from *Michelia formosana* leaf essential oil against wood-rotting fungi. *Molecules*, *27*(7), 2136. DOI: 10.3390/molecules27072136.

Yang, S. Y., Kim, J. H., Su, X. & Kim, J. A. (2022). The luteolinidin and petunidin 3-O-glucoside: A competitive inhibitor of tyrosinase. *Molecules*, *27*(17), 5703. DOI: 10.3390/molecules27175703.

Ye, Z., Chen, D., Zheng, R., Chen, H., Xu, T., Wang, C., Zhu, S., Gao, X., Zhang, J., Li, D., Pang, Y., Zhu, B., Li, Y. & Jia, W. (2021). Curcumin induced G2/M cycle arrest in SK-N-SH neuroblastoma cells through the ROS-mediated p53 signaling pathway. *Journal of Food Biochemistry*, *45*, e13888. DOI: 10.1111/jfbc.13888.

Zagórska-Dziok, M., Bujak, T., Ziemlewska, A. & Nizioł-Łukaszewska, Z. (2021). Positive effect of *Cannabis sativa* L. herb extracts on skin cells and assessment of cannabinoid-based hydrogels properties. *Molecules*, *26*(4), 802. DOI: 10.3390/molecules26040802.